

2
Conf-940529-3

SAND94-0287C

RECEIVED
MAR 21 1994
OSTI

TRACE WATER VAPOR DETECTION IN NITROGEN AND HYDROGEN CHLORIDE GASES BY FTIR SPECTROSCOPY

¹B.R. Stallard, ²L.H. Espinoza, ¹R.K. Rowe, and ²T.M. Niemczyk

¹Sandia National Laboratories
Contamination Free Manufacturing Research Center
Albuquerque, New Mexico, 87185

²University of New Mexico
Department of Chemistry
Albuquerque, New Mexico, 87131

An optical instrument for the determination of trace H₂O in N₂ and HCl gases has been built. It is based on a commercial Fourier transform infrared spectrometer (modified to improve the purge), a long-path gas cell, and classical least squares data analysis. The optimum instrumental parameters have been determined. Particularly important, is the finding that maximal precision is obtained at low resolution, implying that future instruments may be based on less expensive, low-resolution spectrometers. A calibration over the range of 40 to 1800 ppb has been performed and found to be in good agreement with published spectral data. Also, detection limits have been shown to be about 10 ppb. Suggestions are made to improve the design of the instrument.

I. INTRODUCTION

Delivery systems for corrosive gases may be compromised by contamination with even low levels of water vapor. Internal corrosion leads at first to increased particle counts in downstream fabrication tools and later to catastrophic failure. Once corrosion begins, its progress is difficult to arrest since the corrosion itself becomes a moisture source. To extend the life of gas delivery systems and improve wafer yields there is a need for an in-line monitor of H₂O contamination. The goal of this work is to develop an in-line instrument based on FTIR spectroscopy that is compatible with corrosive gases.

DISCLAIMER

MASTER

Se

DISTRIBUTION OF THIS DOCUMENT IS UNLIMITED
Opinions of authors expressed herein do not necessarily state or reflect those of the
United States Government or any agency thereof.

This report was prepared as an account of work sponsored by an agency of the United States Government. Neither the United States Government nor any agency thereof, nor any of their employees, makes any warranty, express or implied, or assumes any legal liability or responsibility for the accuracy, completeness, or usefulness of any information, apparatus, product, or process disclosed, or represents that its use would not infringe privately owned rights. Reference herein to any specific commercial product, process, or service by trade name, trademark, manufacturer, or otherwise does not necessarily constitute or imply its endorsement, recommendation, or favoring by the United States Government or any agency thereof. The views and

II. EXPERIMENTAL

II.1. Instrumentation

Fig. 1 shows the layout of the optical components. The spectrometer is a Nicolet 800 spectrometer operated with a glowbar source (S) and a KBr beamsplitter. The spectrometer, as delivered, has a purge that is inadequate for trace moisture detection. To improve the purge, the entire spectrometer was placed in a polycarbonate box. The deuterated tryglycine sulfate (TGS) detector is used to measure the background water vapor concentration inside the spectrometer, while the indium antimonide (InSb) detector is used to measure the instrument background plus sample water vapor concentration. The strongest H_2O absorption bands in the mid-infrared are centered at approximately 1600 and 3800 cm^{-1} . Based upon the experimental conditions, we chose to use an InSb detector and the 3800 cm^{-1} spectral region for the analysis.

We performed experiments using two different gas cells, as illustrated in Fig. 1. The 22 m multiple-pass White cell (Infrared Analysis Incorporated) is of conventional design with 4" diameter optics enclosed in a 6" diameter Pyrex tube with anodized aluminum end caps. The Axiom cell (Axiom Analytical Incorporated) has eight nickel-coated brass tubes of 2 m length and 1.25" diameter. It has a folded, single-pass design with two 45° mirrors at the end of each tube. The mirror assemblies can be repositioned on the tubes to give a configuration of 2, 4, 6, or 8 tube lengths.

A complete description of the gas handling system is found elsewhere (1). The tubing is 316L stainless steel, seamless, electropolished. The moisture analyzer (Aquamatic Plus by Meeco Incorporated) is used as reference method. A permeation tube (GC Industries) is housed in a L'eau Pro moisture generator (Meeco Incorporated) and is used to generate different amount of water vapor concentrations in N_2 .

II.2 Multivariate Data Analysis

There exist a variety of multivariate techniques for spectroscopic analysis including classical least squares (CLS)(2), partial least squares (3), principal component regression (4), and others (5). CLS was chosen as the appropriate analytic method due to the relative simplicity of our spectroscopic model (1).

Absorption spectra were produced from the sample interferograms without relying on an independent background spectrum. Instead, each interferogram was used to produce its own background spectrum by removing the high frequency information before

performing the Fourier transform. This was achieved by severely apodizing the interferogram with a narrow gaussian function.

Ten regions, encompassing the strongest peaks in the 3800 cm^{-1} region, were chosen for the CLS computation. In each region the CLS algorithm fit the unknown spectrum with the reference spectrum and a linear baseline. This gave a value for the intensity of the unknown spectrum, relative to the reference spectrum in each region. A weighted average of these values gave the final concentration result, where the weighting factors were inversely proportional to the square of the spectral residuals.

III. RESULTS AND DISCUSSION

Fig. 2 illustrates the increase in the precision, or signal to noise ratio (SNR), of the CLS method over the univariate method for a series of resolutions at a fixed collection time. The data are experimental, where the SNR is taken as the ratio of the predicted concentration to the standard error of estimate (SEE) of the prediction for 40 measurements of a slowly varying sample. The univariate results are derived from the peak height of the absorption band at 3837.87 cm^{-1} and based on an analogous calculation for 40 repeated measurements. Experimentally, we see that the improvement of CLS over univariate is from 2 to 5 times. Surprisingly, resolving the narrow H_2O bands ($\text{FWHM} \approx 0.20\text{ cm}^{-1}$) is not necessary to achieve optimal precision. In fact, the greatest precision is achieved at 2 to 4 cm^{-1} resolution, allowing the use an inexpensive interferometer in the final instrument.

A noise analysis was performed to determine the optimum path length of the Axiom cell. The peak of the SNR occurs at a length of 14.5 m. However, in order to better and more quickly attain steady-state conditions within the gas cell, we chose to use a sub-optimal gas cell length of 8 m. It is also of interest to note that in the simplest case, when there is a single detector, the length of the Axiom cell calculated for maximal SNR is 6.2 m (1).

Fig. 3 plots the H_2O concentration in N_2 determined spectroscopically versus the concentration determined by the reference method, using the Axiom gas cell and a range of concentrations from 40 to 320 ppb. The inverse of the slope of the best-fit line gives a calibration for the arbitrary CLS units, which is 106.3 ppb per CLS unit (standard error = 7.1 ppb). We repeated the calibration with the White cell using somewhat greater levels of H_2O (i.e., 150 - 1800 ppb), and found a value of 44.1 ppb per CLS unit (standard error = 1.1 ppb). Adjusting the White cell results to an 8 m path yields an equivalent calibration of 121.2 ppb per CLS unit (standard error = 2.9 ppb). Although reasonably close, the two calibration results may differ due to systematic errors (1). The data may also be presented in the form of cross-validated calibration plots. In such a

case, the standard error of prediction (SEP) is equivalent to the measurement error. In this way, we determined that the errors for the experiments were 18 ppb using the single-pass Axiom cell, and 48 ppb using the multi-pass White cell (1).

The concentration of H_2O was determined by two separate measurements of 10 minutes each: first, the instrument background plus sample (InSb detector), and second, the instrument background alone (TGS detector). The final concentration estimate was then calculated as the difference between the concentration values produced from these two measurements. The error in the individual InSb and TGS concentration values were determined by 54 repeated measurements on a stable sample of H_2O in N_2 over a nine-hour period. Since a small amount of drift (about 10 ppb, in this case) was unavoidable, the SEE was used as the measure of precision, where the drift was modeled by a second order polynomial. The SEE's are: 3.3 ppb for InSb, and 9.1 ppb for TGS, using a pathlength of 8 m. The background determination was less precise due to the choice of the noisier TGS detector for this task, which was chosen because the present experimental setup does not permit a liquid nitrogen cooled detector to monitor the spectrometer background. The measurement precision for H_2O in HCl was determined from a similar set of repeated measurements, as illustrated in Fig. 4, which was collected with approximately 100 ppb H_2O in HCl within the 8 m Axiom cell. In this case, the InSb SEE is 8.4 ppb, which is poorer than the corresponding nitrogen value due to the effect of the interfering species, CO_2 and CH_4 , in HCl. Also, the preceding analysis is based upon the assumption that the calibration for low levels of H_2O in HCl is identical to the calibration for H_2O in N_2 . This point has been addressed in the literature (6,7) and will be the subject of future investigation.

From the errors determined experimentally (18 ppb for the low range calibration; 3.3 ppb due to InSb, and 9.1 ppb due TGS) the residual error is calculated as follows:

$$\sigma_{\text{res}} = [18 \text{ ppb}^2 - 3.3 \text{ ppb}^2 - 9.1 \text{ ppb}^2]^{1/2} = 15.2 \text{ ppb}$$

This error is consistent with the specified performance of the reference method. Following an analogous calculation for the high range calibration (not shown) (1), the residual is found to be 48.0 ppb. While the error of the reference method must be near 15 ppb for this case also, there is the added problem of attaining adequate equilibrium with the White cell. Errors due to the difficulty in achieving equilibrium are indistinguishable from errors due to the reference method and may explain the higher residual error. Considering only the errors from the FTIR system, it appears that the detection limits for the current instrument are: 9.7 ppb ($\sigma_{\text{InSb}} = 3.3 \text{ ppb}$, $\sigma_{\text{TGS}} = 9.1 \text{ ppb}$) for H_2O in N_2 , and 12.4 ppb ($\sigma_{\text{InSb}} = 8.4 \text{ ppb}$, $\sigma_{\text{TGS}} = 9.1 \text{ ppb}$) for H_2O in HCl.

From the calibration discussed above it is possible to derive an absorptivity for each H_2O band in the spectrum. The absorptivities found in this work (using 106 ppb per CLS unit) were compared with those published in the HITRAN data base (8). We found that

our measured values were typically 77% of those derived from HITRAN.

IV. DESIGN IMPROVEMENTS

The current mechanism for switching between sample and background measurements is slow and requires that all the scans for one measurement be completed before beginning the other. A new design will use a single InSb detector with two nearly identical beam paths to alternately collect the sample and background interferograms, at about one scan per second. This minimizes the effect of the background drift and avoids the use of the low performance TGS detector.

Significant improvement in the SNR can be realized through the use of optical and electronic filters. A redesigned system will use an optical bandpass filter to limit the light incident on the detector to only those spectral frequencies of interest, allowing us to boost the signal while avoiding detector saturation (1). Also, during the current set of experiments, the electronic bandpass filters of the spectrometer were set to collect spectra from 0 to 7900 cm^{-1} . Since we are interested in only a small portion of the spectrum, the electronic pass band can be trimmed significantly, greatly reducing the amount of noise at other electronic frequencies (1).

The current implementation of the CLS algorithm considers only a single component, H_2O , in addition to a linear baseline. However, semiconductor grade HCl can have a significant amount of other gases that absorb in the 3600 to 3900 cm^{-1} region. For example, the HCl used in these experiments has a specified limit of 10 ppm for CO_2 , and 2 ppm for CH_4 . In the future, a three-component CLS analysis will be used, which should improve the H_2O estimate, and will provide simultaneous information on CO_2 and CH_4 impurity levels (1).

With these enhancements, it will be possible to shorten the collection time substantially and still maintain a detection limit superior to the present instrument. We project that a redesigned instrument with the foregoing enhancements will have a detection limit of better than 1 ppb, using a one minute data collection time (1).

ACKNOWLEDGEMENTS

This work was performed at Sandia National Laboratories and the University of New Mexico, and was supported jointly by the U.S. Department of Energy under Contract Number DE-AC04-94-AL85000, and by SEMATECH.

REFERENCES

1. B.R. Stallard, R.K. Rowe, L.H. Espinoza, M.J. Garcia, T.M. Niemczyk, and D.M. Haaland, "Trace Water Vapor Determination in N_2 and HCl by Infrared Spectroscopy," *Report SAND 93-4026*, Dec. 1993 (available through Sandia National Laboratories).
2. D.M. Haaland and R.G. Easterling, *Appl. Spect.*, **34**, 539 (1980). (Note that there are some typographical errors in the mathematical expressions in this paper.)
3. M.P. Fuller, G.L. Ritter, and C.S. Draper, *Appl. Spect.*, **42**, 217 (1988).
4. D.M. Haaland, R.G. Easterling, and D.A. Vopicka, *Appl. Spect.*, **39**, 73 (1985).
5. E.V. Thomas and D.M. Haaland, *Anal. Chem.*, **62**, 1091 (1990).
6. D. Pivonka, *Appl. Spect.*, **45**, 597, 1991.
7. Miyazaki, Y. Ogawara, and T. Kimura, *Bull. Chem. Soc. Jpn.*, **66**, 969, 1993.
8. L.S. Rothman, R.R. Gamache, R.H. Tipping, C. P. Rinsland, M.A.H. Smith, D.C. Benner, V.M. Devi, J.M. Flaud, C. Camy-Peyret, A. Perrin, A. Goldman, S.T. Massie, L.R. Brown, and R.A. Toth, *J. Quant. Spectr. Radiat. Transfer*, **48**, 469 (1992).

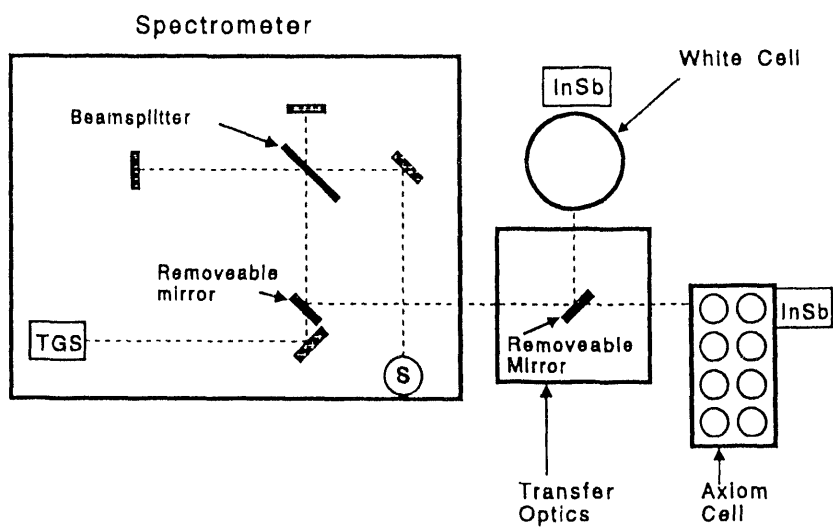


Fig. 1: System Schematic

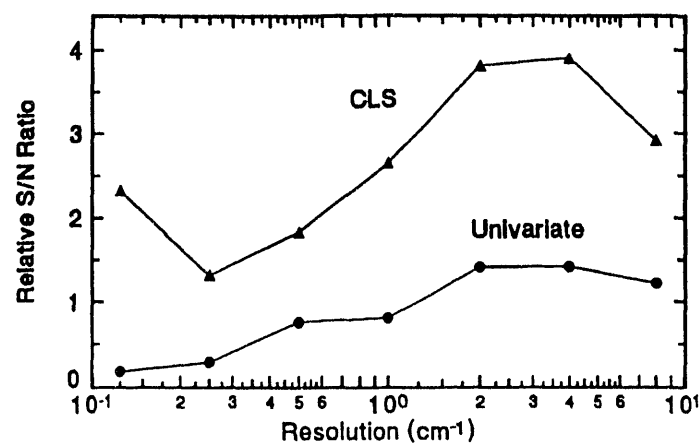


Fig.2: Experimental Signal to Noise Ratio vs. Resolution

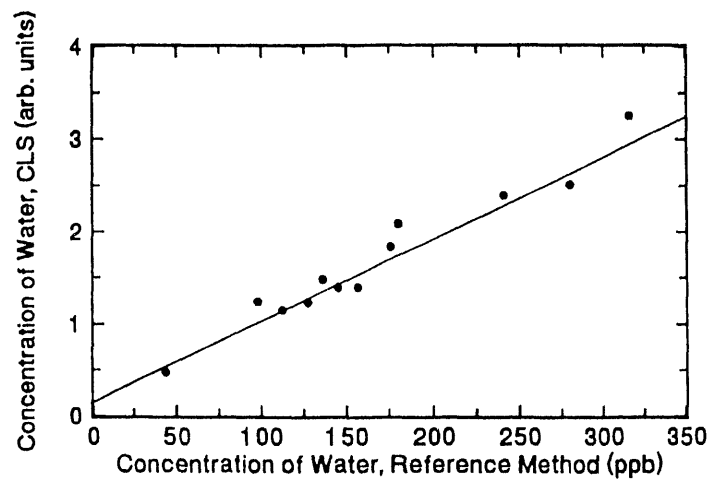


Fig.3: Measured vs References Values, H_2O in N_2 , Axiom Cell

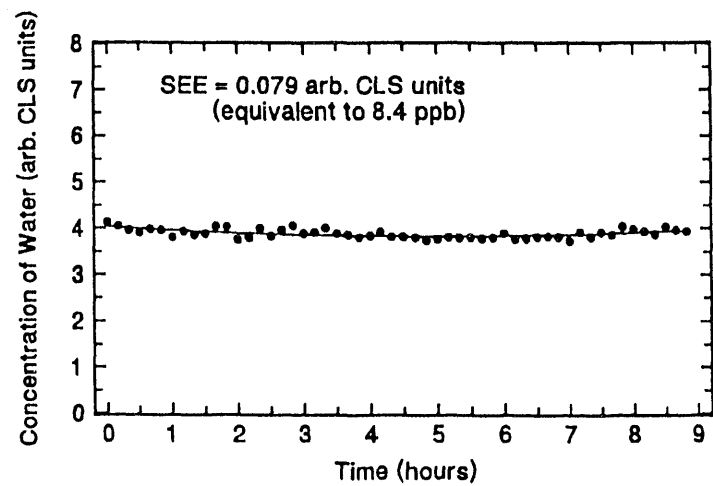


Fig.4: Measurement Precision of H_2O Concentration in HCl

A vertical stack of three abstract black and white shapes. The top shape is a horizontal rectangle divided into four vertical segments of varying widths. The middle shape is a trapezoid pointing downwards, with its top edge being a horizontal line. The bottom shape is a large, irregular, rounded rectangle with a white U-shaped cutout in its center.

High

תְּלִמְדָּיִם

DATA

